accurate to 0.27 arcsec as long as $\Delta\phi$ and $\Delta\lambda$ are each less than 7 arcmin. Thus, level deviations (<7 arcmin) in latitude can be ignored and the correction for longitude level effects is quite simple.

Required Positional Accuracy

From the preceding paragraph it can be seen that to the azimuth uncertainty derived from individual star transits will be added errors caused by lack of positional knowledge in applying the correction there derived. From Eq. (A5), the variance $\epsilon^2(\Delta\theta)$ in the correction $\Delta\theta$ is

$$\epsilon^2(\Delta\theta) = \cos^2\phi\ \epsilon^2(\Delta\lambda) + (\Delta\lambda)^2 \sin^2\phi\epsilon^2(\phi)$$

Let us take the second term first. As said above, $\Delta\lambda$ has a maximum value of 7 arcmin and $\phi \sim 45°$. For the second term to contribute less than 0.2 arcsec to $\Delta\theta$, $\epsilon(\phi)$ cannot exceed

$$0.2 \text{ arcsec}/(7 \text{ arcmin} \times 0.707) = 2.3 \text{ arcmin}$$

Thus, latitude of the site need only be known to about two miles.

The first term is due to longitude uncertainties. Again, for $\phi \sim 45°$ and $\epsilon(\Delta\theta) < 0.2$ arcsec, $\epsilon(\Delta\lambda)$ cannot exceed $0.2/0.707 = 0.28$ arcsec. Thus, longitude must be known to better than 30 ft, and corresponding clock errors must be kept below a similar number of milliseconds.

References

[1] Berg, R. T., "Measurement of the Astronomic Azimuth of a Mirror Normal," Test Pad Stability Symposium No. 4, May 15–16, 1963, Honeywell, Inc., Minn.

[2] Pavlov, N. N., "The Photoelectric Registration of Star Transits," *Publications of the Central Observatory at Pulkova*, Ser. II, Vol. LIX, Leningrad, 1946.

[3] Liang, T.-Y., "Determination of Time, Longitudes, Latitudes and Azimuths by the Photoelectric Method," *Geodesy and Aerophotography*, No. 1, 1963, pp. 32–38.

[4] Moreau, R. L., "Photoelectric Observations in Geodetic Astronomy," *Canadian Surveyor*, Vol. 20, No. 4, 1966, pp. 282–291.

[5] Abby, D. G., "Development of an Electro-Optical Theodolite," XI Pan American Consultation on Cartography, 1969, Pan American Institute of Geography and History, Washington, D.C.

[6] Carroll, J. E., "A New Instrument for the Determination of Astronomic Position," *Surveying and Mapping*, Sept. 1969, Vol. XXIX, No. 3, pp. 447–461.

[7] *Smithsonian Astrophysical Observatory Star Catalog*, Smithsonian Publication 4652, Supt. of Documents, U.S. Government Printing Office, Washington, D.C. 20402, 1966.

[8] Berg, R., private communication, July 1969, Honeywell, Inc., Minneapolis, Minn.

NOVEMBER 1970 J. SPACECRAFT VOL. 7, NO. 11

Reaction-Boom Attitude Control Systems

W. W. Hooker,* I. P. Leliakov,† M. G. Lyons,‡ and G. Margulies§
Lockheed Missiles & Space Co., Sunnyvale, Calif.

Active gravity-gradient stabilization systems are shown to permit significant improvement in the stabilization and maneuvering capability of Earth-pointing satellites compared to more conventional momentum storage and mass expulsion techniques. The proposed configuration consists of the payload body and a properly arranged array of gimballed "reaction booms." The appropriate boom gimbals are torqued on the basis of payload attitude and gimbal sensor data. Qualitatively, the system may be viewed as a hybrid that derives rapid momentum transfer and payload maneuvering capability from active torquing between the component parts of the satellite, while obtaining the necessary momentum dumping from gravity-gradient torques acting on the over-all configuration. The number, geometry, and hinging of the booms is dependent on the specific control or maneuvering requirements; therefore, three distinct system types are proposed. Procedures for selecting control laws are developed on the basis of simplified dynamic models, and the expected system performance is verified through simulation of both linearized and full nonlinear system models. The observed payload response resembles that of a fast reaction-wheel system. Low-frequency, gravity-gradient modes are effectively decoupled from payload motion and boom oscillations are satisfactorily constrained even for large-angle payload steering maneuvers.

Nomenclature

c_i = damping coefficient
$\bar{E}_i$ = orbiting reference axes, i = 1,2,3
$\bar{e}_i$ = payload body axes, i = 1,2,3
f,g $\equiv 4\Omega^2$ and $3\Omega^2$, respectively
θ_i = main body roll, pitch, yaw angles with respect to the orbiting reference axes, i = 1,2,3
α_i,β_i = relative roll and pitch boom gimbal angles for the i^{th} boom, i = 1,2,3,4
H_i = momentum of reaction wheel aligned with $\bar{e}_i$, i = 1,2,3
I = payload moments of inertia
J = reduced moments of inertia of one boom (about axis normal to boom and relative to composite system CM)
k = spring coefficient
T_i' = torque on reaction wheel parallel to $\bar{e}_i$, i = 1,2,3
$T_{\alpha i}',T_{\beta i}'$ = torques on the α and β gimbals of the i^{th} boom,¶ i = 1,2,3,4
Ω = mean orbit rate
ω_n = natural frequency
ζ = damping ratio

Received September 11, 1969; revision received August 12, 1970.

* Research Scientist, Mathematics & Operations Research Laboratory.
† Staff Engineer, Guidance & Flight Mechanics Department.
‡ Senior Research Engineer, Attitude Stability & Control Systems Department. Member AIAA.
§ Senior Staff Scientist, Mathematics & Operations Research Laboratory.

¶ For configurations A and B, i = 1.

Introduction

THE term "reaction boom" is used herein as a generic term to describe an extendible structure attached to a spacecraft by means of a set of steerable gimbals. Active attitude control systems can be designed to incorporate such reaction booms in a variety of ways. Their use represents a logical outgrowth of present-day technology. To illustrate the applicability of such systems to a variety of Earth-satellite pointing and maneuvering missions, several conceptual implementations will be presented and discussed.

For reference, let us note that current high-performance attitude-control systems that are required to perform pointing, tracking, and maneuvering functions with sensor-limited accuracy generally utilize reaction wheel arrays as primary actuators. The latter are augmented with a discontinuous mass expulsion mechanisms, whose main on-orbit function is the occasional unloading of the wheels as these approach angular momentum saturation. The following basic drawbacks of this approach are well-known: 1) tracking and slewing maneuvers, performed with the usual low-inertia, high-speed reaction wheels, are characterized by high power consumption and low efficiency, and auxiliary use of mass expulsion systems results in rapid increase of propellant weight and the number of valve actuations; 2) reaction wheels are high-speed devices and have correspondingly short life expectancies ($\leq$5 yr); and 3) because of over-all complexity, reliable implementation generally requires redundancy of equipment and increased system weight.

For missions requiring relatively limited control system capability, these difficulties frequently have been circumvented by the use of specialized control systems (e.g., dual-spin and control moment gyros) that optimize certain system characteristics at the expense of others. However, requirements on control system performance and life expectancy are becoming more stringent, and there exists a growing need for a more comprehensive solution.

An examination of items 1, 2, and 3, together with the observation that the basis of control, from a dynamical point of view, lies in the controlled interchange of angular momentum between the wheels and the payload, suggests the concept of a reaction boom. For a given required level of angular momentum, the high speed of the wheels is an unavoidable consequence of their low inertia; moreover, the symmetry in mass distribution of a wheel minimizes any angular momentum interaction with the external gravity-gradient torque field. Whereas in a reaction-wheel control system design the gravitational field is a source of disturbance torques to be corrected, the reaction-boom design exploits the gravity-gradient field to provide a mechanism that eliminates the problem of angular momentum saturation and the requirement for momentum dumping via mass expulsion. By appropriately orienting steerable reaction-booms in the gravitational field, small deflections of the gimbals can be used to give rise to controlled, continuously-acting gravity-gradient torques on the over-all satellite to counteract the accumulation of error angular momentum due to various disturbance torques. As a control element, the reaction-boom can thus be viewed as equivalent to a generalized large reaction wheel with a built-in momentum unloading mechanism. It is important to observe that this utilization of booms is quite different from that of coarse, passive gravity-gradient control systems, since minute gravitational torques are not utilized to control the attitude of the payload, but serve only as a passive mechanism for preventing the secular build-up of error angular momentum on the satellite. In this mode of operation, the critical nature of static boom straightness, thermal bending, and other slow deformations is considerably reduced.

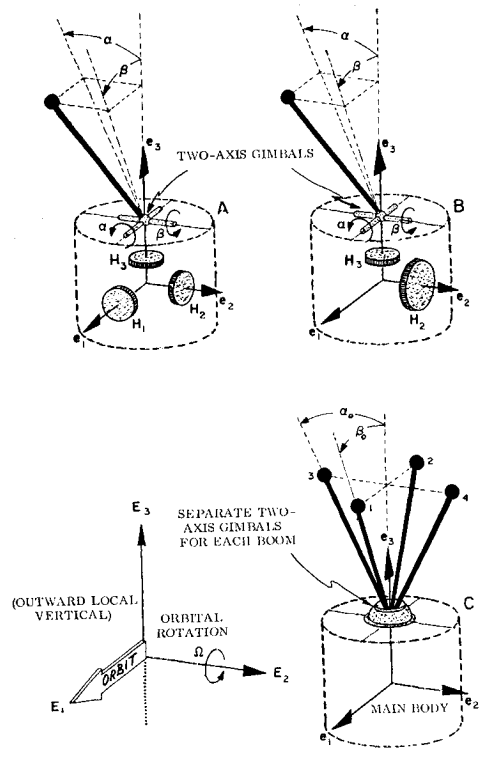

Fig. 1 System configurations and reference frames.

The feasibility of reaction-boom control for a specific configuration has been demonstrated.[1,2] Hence, much of the present treatment is aimed at generalizing the essentials of system selection and design.

For purposes of this paper, the operation of the active control loops is taken to be continuous and linear, with the exception of discrete gimbal rate computation and gimbal stops in the large-angle simulation studies. Multiply-hinged, rigid-body models are used to describe the over-all satellite attitude dynamics. In practice, boom deformation effects will influence system performance. However, the relative insensitivity of reaction-boom systems to changes in boom geometry at frequencies within the bandwidth of the gimbal servos makes it possible to relegate this problem to the level of detailed design.

The number of possible configurations using reaction booms and momentum wheels in various combinations is quite large. The choice of any particular system must be made on the basis of performance requirements and design constraints associated with a given mission. We will consider three representative configurations.

The first proposed application[1,2] of a reaction boom in an augmenting role is that shown as configuration A of Fig. 1. The system contains a 3-axis reaction-wheel array, control electronics, and 3-axis attitude sensing. A single reaction boom, gimballed about two axes, replaces the usual 3-axis mass expulsion backup system. As shown in the analysis of the configuration, proper utilization of the boom dynamics may be used to provide both momentum unloading and steering capability for the payload body. From the viewpoint of control system weight and power requirements, this configuration can be shown to be superior to the traditional wheel-gas systems for long-life applications.

Configuration B is a further example of reaction-boom augmentation. The original system (without a boom), containing two wheels, Earth sensing, and either a mass expulsion or magnetic torquing scheme for wheel unloading, was proposed by Terasaki.[3] The configuration derives yaw stability from passive gyroscopic torques obtained by operating the pitch wheel with a fixed speed bias. Pitch control and maneuvering are achieved by modulating the bias speed. Roll maneuvering and control are obtained by operating the yaw reaction wheel. The concept is unique in that it allows three-axis stabilization and two-axis attitude maneuvering without the usually combersome active yaw sensing. The re-

placement of the traditional momentum dumping systems with a single reaction boom leads to significant improvement in system characteristics. Over-all weight and maneuvering power requirements are reduced, while the system response rates to steering commands can be increased through appropriate boom gimbal torquing.

Configuration C approaches an optimum in reaction boom utilization. It requires 3-axis sensing and control electronics and uses reaction booms as the only control actuators. Two gimballing mechanizations are possible, leading to somewhat different dynamic characteristics. One arrangement using separate 2-axis gimbals for each boom yields a 5-body system. An alternative approach consists of rigidly connecting the "in-plane" booms (1 and 2) and the "out-of-plane" booms (3 and 4) to obtain two rigid V-shaped pairs, and attaching each pair to the payload by means of a 3-axis gimbal system. The performance capability, as well as the associated small-angle dynamics analysis and control law selection procedures, parallel closely those of configuration A. Hence, a quantitative treatment of configuration C is omitted.

The choice between A and C can, in general, be made only on the basis of specific equipment requirements. However, both configurations offer significant mechanization advantages over wheel-only systems (e.g., maneuvering power and system weight for long-life missions are significantly reduced). The most promising feature of C may be its potential for extremely long life. In the absence of high-speed rotating parts, valves, etc., and with suitable mechanization of the gimbals (e.g., using flexure pivot suspensions), control actuators of this type may be capable of 10- to 20-yr life.

Dynamical Models

Configurations A, B, and C can be represented by a common dynamic model of several rotationally interconnected rigid bodies. Available dynamic attitude equations for multi-body satellites in the gravitational field[4] were used in this study both for the derivation of linearized equations of motion[5] and for the development of a full nonlinear large-angle computer simulation program capable of representing configurations A, B, and C. Because of the length and complexity of these equations,[5] they will not be reproduced here.

Linear Analysis

Qualitatively, a reaction boom may be viewed as an inertially large and gravitationally stable platform, to which a relatively smaller payload body is attached by means of a set of gimbals. Active control of the gimbals with fast-response servos provides accurate pointing of the payload, at the expense of motion of the reaction boom(s). Because of its relative size and mass distribution, the reaction boom always remains in the vicinity of its gravitational equilibrium attitude and undergoes only small librational motions as a result of gimbal torques and external disturbances. The motion of a "rigid" reaction boom will, in general, contain modes at the natural frequencies of the gimbal servos, and the usual low-frequency libration modes associated with the motion of passive gravity-stabilized configurations. To obtain fast response characteristics for the payload, the active control law must be selected so as to decouple the motion of the payload from the low-frequency boom librations. As demonstrated later, this control law is realized by orienting the torque axes of the control actuators (i.e., wheels and booms) so that the attitude dynamics model for each control axis becomes that of (at least) a 3-body system. In effect, the momentum transfer associated with the gravitational librations is forced to bypass the payload and takes place only between the two control actuators. Provided that the boom motion is reasonably bounded, the slow damping of these modes is quite acceptable since payload response remains unaffected.

To illustrate the selection of the control laws for configurations A and B, the dynamic models of these systems have been simplified to retain only those features essential to demonstrating system performance. In this sense, it is advantageous to consider only rigid structures having simple moments of inertia. Thus, the payload body is taken to be spherical, and the gimbal array is placed at the center of mass of the payload. The booms are assumed to be rigid and massless, with point tip masses. It is understood that practical deviations from these simplifications will lead to changes in both the system models and the control law selection. However, these modifications make the proposed approach no less applicable.

Configuration A

Based on the modeling procedures and using the normalizing substitutions

$$T_{xx} = T_{xx}'/I,\ h = H_i/I,\ r = I/J \tag{1}$$

the system small-angle equations are found to be:

$$\ddot{\theta}_2 = T_2 + T_\beta \tag{2}$$

$$\ddot{\theta}_2 + g\theta_2 + \ddot{\beta} + g\beta = -rT_\beta \tag{3}$$

$$\ddot{\theta}_1 + \dot{\theta}_3\Omega + h_3\Omega = T_1 + T_\alpha \tag{4}$$

$$\ddot{\theta}_3 - \dot{\theta}_1\Omega - h_1\Omega = T_3 \tag{5}$$

$$\ddot{\theta}_1 + \theta_1 f + \ddot{\alpha} + \alpha f = -rT_\alpha \tag{6}$$

$$\dot{h}_i = -T_i,\ (i = 1,2,3) \tag{7}$$

The control law selection procedure is best exemplified by the pitch mode Eqs. (2), (3), and (7).

Although it is possible to prescribe a variety of control characteristics for the payload body, let it be assumed that the payload pitch (θ_2) response is to be that of a second-order system with a natural frequency ω_n and a damping ratio ζ. Inspection of Eq. (2) yields the requirement $T_2 + T_\beta = -k_1\theta_2 - c_1\dot{\theta}_2$.

The remainder of the control law is to be chosen to insure damping of the remaining system modes, and to prevent excessively high amplification of motion for steady-state excitation at the usually critical orbital and twice-orbital frequencies. Assuming that the entire state vector is available for measurement, a general candidate control law which does not increase the order of the system is**

$$T_\beta = -k_1\theta_2 - c_2h_2 + c_3\dot{\beta} \tag{8}$$

$$T_2 = -c_1\dot{\theta}_2 + c_4h_2 - c_5\dot{\beta} \tag{9}$$

Some obvious guidelines for the selection of $c_2, \ldots, c_5$ are found by examining the characteristic equation, viz.,

$$\begin{vmatrix} (s^2 + sc_1 + k_1) & s(c_5 - c_3) & (c_2 - c_4) \\ (s^2 + g - rk_1) & s^2 + src_3 + g & -rc_2 \\ (-sc_1) & (-sc_5) & (s + c_4) \end{vmatrix} = 0 \tag{10}$$

Note that the first row of the determinant, representing the payload motion, decouples from the system only for $c_3 = c_5$, $c_2 = c_4$. Furthermore, the remainder of the system is damped and wheel speed is bounded if and only if $c_1, c_2, c_3 \neq 0$. The selection of c_2 and c_5 is not critical and is readily performed through the use of root-locus methods or numerical means, by considering only the cofactor of the $(s^2 + sc_1 + k_1)$ term. The range for both c_2 and c_5 of $(g)^{1/2} \leq c < (10g)^{1/2}$ is found to give satisfactory characteristics.

** Note that in accordance with the earlier discussion the boom is used to provide the restoring or steering component of control torque, while the wheel acts primarily as an active damper.

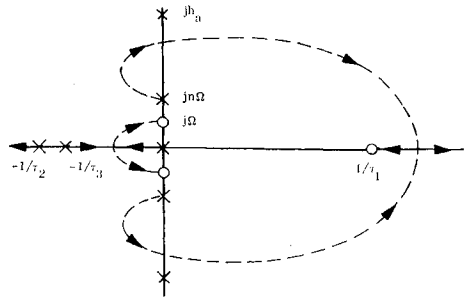

Fig. 2 Root locus of $P(s)$ vs k_2.

The boom-wheel system is of third order and, for light damping, has a resonant peak near $\omega \cong (g)^{1/2} = \Omega(3)^{1/2}$. The payload body response is that of a second-order system of $\omega_n = (k_1)^{1/2}$, $\zeta = c_1/2(k_1)^{1/2}$. Note that the bandwidth of the payload loop is limited by the maximum value of k_1 which may be used in the control law Eq. (8), without producing excessively high moments on the boom structure. Typical attainable payload performance characteristics are in the range $10\Omega \leq \omega_n \leq 100\Omega$ with $\zeta = 0.7$. The associated "$1/e$ decay time" of the least damped boom/wheel mode is of the order of 10 orbital periods. The associated steady-state response characteristics are discussed later.

Briefly considering the roll-yaw dynamics of configuration A, Eqs. (4-7) and control laws of the form

$$T_1 = -c_1'\dot{\theta}_1 + c_2'h_1 + c_5'\dot{\theta}_3 - c_4'\dot{\alpha} + h_3\Omega \quad (11)$$

$$T_\alpha = -k_1'\theta_1 - c_2'h_1 + c_4'\dot{\alpha} \quad (12)$$

$$T_3 = c_6'\dot{\theta}_3 - k_6'\theta_3 + c_7'\dot{\theta}_1 - h_1\Omega \quad (13)$$

yield an 8th-order characteristic equation of the system. The selection of the control law begins by decoupling roll and yaw by setting $c_7' = -\Omega$, $c_5' = \Omega$.

Subsequently, the second-order response characteristics (or any other desired response) for the payload roll and yaw axes may be selected: $\omega_{n_1} = (k_1)^{1/2}$, $\zeta_1 = c_1'/2(k_1')^{1/2}$, $\omega_{n_3} = (k_6')^{1/2}$, $\zeta_3 = c_6'/2(k_6')^{1/2}$.

The remainder of the system can be damped by $c_2' \neq 0$, $c_4' \neq 0$. The undamped system oscillates at $\omega = \Omega$ and $\omega = 2\Omega$. Since external perturbations commonly appear at these frequencies, the numerical selection of c_2' and c_4' must consider not only the decay rates of the two modes, but also the positions of the resonance peaks in the system frequency response characteristics. Numerical root-locus calculations show that values

$$c_2' \cong 1.4\Omega,\ c_4' \cong 10\Omega \quad (14)$$

yield acceptable damping times and prevent excessive amplification of steady-state boom and wheel motion at $\omega = \Omega$ and $\omega = 2\Omega$. Representative frequency response characteristics are discussed in more detail later.

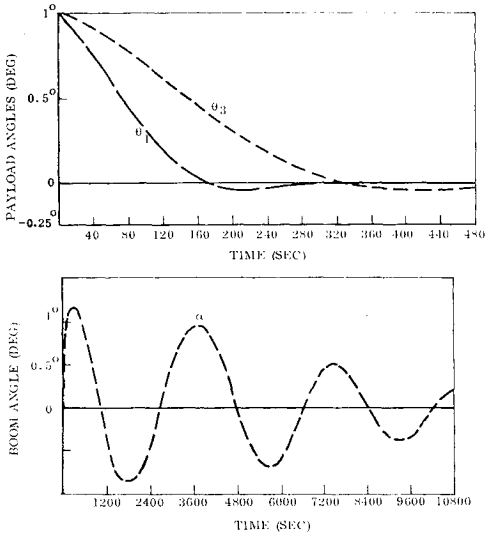

Fig. 3 Transient response of configuration A to initial error, $\theta_{1,3} = 1°$ (linear solution).

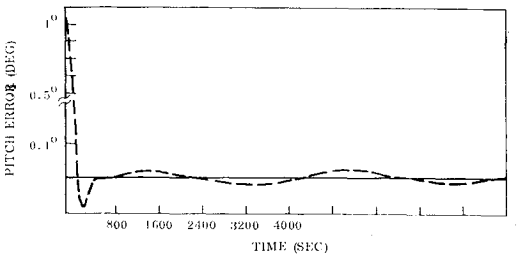

Fig. 4 Transient response of configuration A to initial error $\theta_2 = 1°$, for $(c_3 - c_5) = 0.1\ c_1$ (linear solution).

Configuration B

The small-angle model of the attitude dynamics of the 2-wheel configuration shows, as expected, that pitch and roll-yaw motions are described by two decoupled sets of equations. Moreover, the structure of the pitch model is identical to that of configuration A, and hence requires a corresponding parallel control law selection procedure. The roll-yaw system characteristics differ from those of configuration A in that the available torque actuators have more limited capability. Here yaw stability is achieved with a pitch angular momentum bias. Hence one expects more interaxis coupling, as well as somewhat reduced performance from the final system design. As will be shown, configuration B also requires a more intricate control law selection process for the roll-yaw axes.

Redefining the pitch wheel angular momentum H_2 as the sum of variable component H_2' and a constant component H_a, the small-angle roll-yaw model of the system becomes (for $H_a/I \equiv h_a$)

$$\ddot{\theta}_1 + h_a\Omega\theta_1 + \dot{\theta}_3(\Omega - h_a) + \Omega h_3 = T_\alpha \quad (15)$$

$$\ddot{\theta}_3 + h_a\Omega\theta_3 - \dot{\theta}_1(\Omega - h_a) = T_3 \quad (16)$$

$$\ddot{\theta}_1 + f\theta_1 + \ddot{\alpha} + f\alpha = -rT_\alpha \quad (17)$$

$$\dot{h}_3 = -T_3 \quad (18)$$

Since payload yaw attitude and rate are not sensed, neither T_α nor T_3 may contain terms derived from θ_3. Hence, the payload roll motion of Eq. (15) may not be decoupled from yaw, except for the small value of $h_a = \Omega$. At the same time, the primary yaw restoring mechanism consists of passive gyroscopic torques proportional to the pitch wheel bias mo-

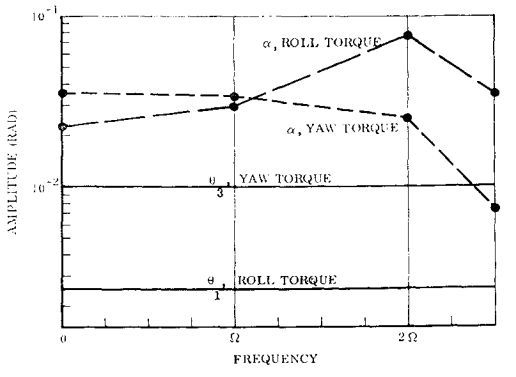

Fig. 5 Steady-state response amplitudes of configuration A to torque on payload $T = I \times 10^{-6} \sin(n\Omega t)$ (ft-lb).

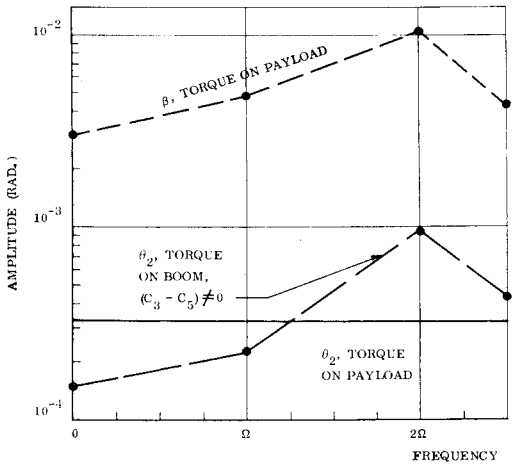

Fig. 6 Steady-state response of configuration A to pitch torque $T = I \times 10^{-6} \sin(n\Omega t)$(ft-lb).

mentum. Thus, to minimize the over-all system response times, and to stiffen the yaw axis to external disturbances, it is desirable to use a large value of h_a. Furthermore, it is essential to ensure rapid decay of the associated passive mode, since it will inherently appear in both the yaw and roll response characteristics.

In selecting the components of T_α, it is recalled that a term proportional to θ_1 is required for rapid response and efficient roll torquing. Also, inspection of Eq. (17) shows that the introduction of a viscous torque term $c_2\dot{\alpha}$ is the only means available to damp the passive gravity-gradient boom mode at $\omega = (f)^{1/2} = 2\Omega$. With these necessary ingredients T_α becomes

$$T_\alpha = -k_1\theta_1 + c_2\dot{\alpha} \tag{19}$$

Assuming a general control law for T_3 of the form

$$\hat{H}_3(s) = \Theta_1(s)F(s) + \mathfrak{A}(s)G(s) \tag{20}$$

where $\hat{H}_3(s) = \mathfrak{L}h_3(t)$ and $\mathfrak{A}(s) = \mathfrak{L}\alpha(t)$ the system characteristic equation becomes

$$\begin{vmatrix} (s^2 + h_a\Omega + k_1) & s(\Omega - h_a) & (-sc_2) & \Omega \\ -s(\Omega - h_a) & (s^2 + h_a\Omega) & 0 & s \\ (s^2 + f - rk_1) & 0 & (s^2 + src_2 + f) & 0 \\ -F(s) & 0 & -G(s) & 1 \end{vmatrix} = 0 \tag{21}$$

It is seen that for $G(s) = 0$, $c_2 = 0$, the motion of the payload becomes decoupled from the passive boom libration.

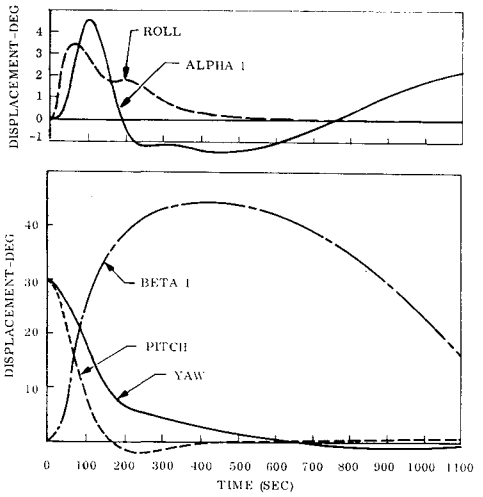

Fig. 7 Transient response of configuration A to initial error $\theta_2 = \theta_3 = 30°$ (no gimbal stops).

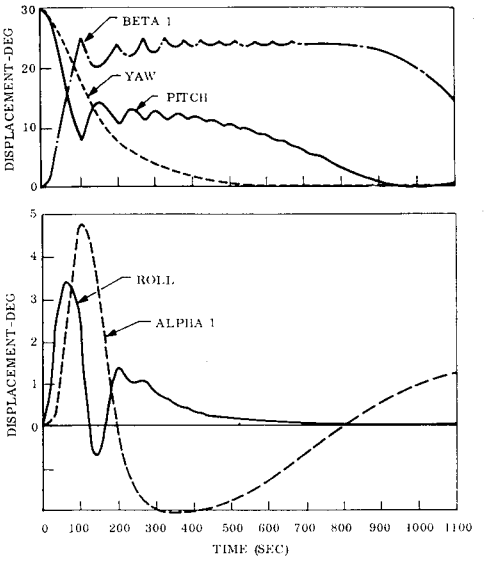

Fig. 8 Transient response of configuration A to initial error $\theta_2 = \theta_3 = 30°$ (with gimbal stops).

A possible strategy thus is to use the minimum value of c_2 required to damp the boom mode, and to derive T_3 only from roll (θ_1) attitude. In fact, c_2 may be temporarily kept at zero to facilitate the selection $F(s)$. The decoupled payload roll-yaw system $P(s)$ then becomes the cofactor of the $(s^2 + src_2 + f)$ term of Eq. (21)

$$P(s) = \begin{vmatrix} (s^2 + h_a + k_1) & s(\Omega - h_a) & \Omega \\ -s(\Omega - h_a) & (s^2 + h_a\Omega) & s \\ -F(s) & 0 & 1 \end{vmatrix} = 0 \tag{22}$$

The root structure of $P(s)$ as a function of h_a and k_1 is readily obtained through standard numerical root-locus computations. It is found that in the practical range of parameters

$$10\Omega < h_a < 100\Omega,\ k_1 < 100\Omega^2 \tag{23}$$

the stability of $P(s)$ may be obtained by taking

$$F(s) = k_2(\tau_1 s - 1)/(\tau_2 s + 1)(\tau_3 s + 1) \tag{24}$$

The role of the critical frequencies of $F(s)$ is best illustrated in the schematic root locus of $P(s)$ versus k_2 shown in Fig. 2, as computed from the form

$$P(s) = 1 + \frac{k_2 h_a \tau_1 (s - 1/\tau_1)(s^2 + \Omega^2)}{\tau_2\tau_3 s(s + 1/\tau_2)(s + 1/\tau_3)(s^2 + n^2\Omega^2)(s^2 + h_a^2)} \tag{25}$$

The position of the roots $\pm jn\Omega$ is determined by the choice of k_1 and h_a, and for the range of Eq. (23) becomes $3 < n < 9$.

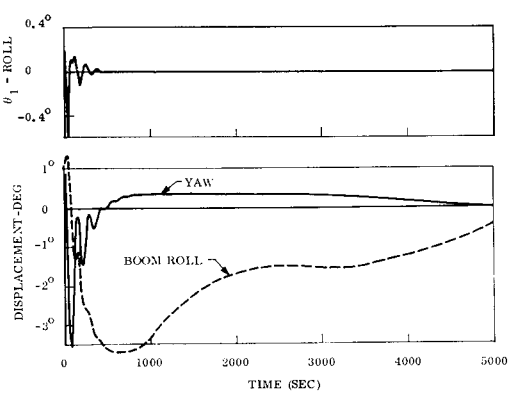

Fig. 9 Transient response of configuration B to initial error $\theta_1 = 1°$ (linear solution).

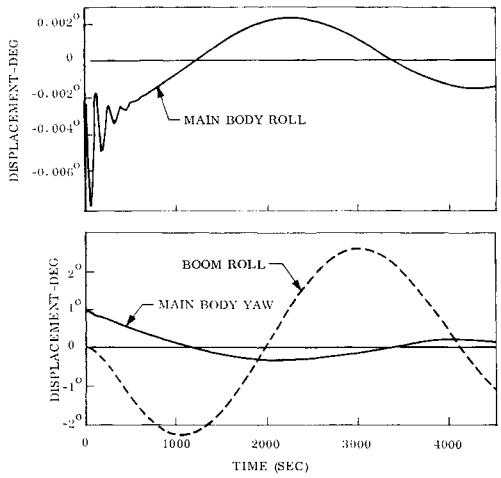

Fig. 10 Transient response of configuration B to initial error $\theta_3 = 1°$ (linear solution).

Figure 2 shows a suitable stable region of $P(s)$ for a range of k_2. The final step in the control law selection is the numerical root-locus computation for the overall system as a function of c_2. Representative values obtained with the above procedure are found to be

$$h_a \cong 100\Omega \qquad \tau_1 \cong \tau_2 \cong \tau_3 \cong 1/h_a$$

$$k_1 \cong 4 \times 10^4\Omega^2 \qquad k_2 \cong 0.2 \times 10^4\Omega^2$$

$$c_2 \cong 20 \times 10^{-3}\Omega$$

Performance, Analysis and Simulation

To summarize the observed performance characteristics, a number of selected examples are presented for each configuration. These include computed small-angle transient responses, linear frequency-response characteristics, and digital computer simulation of large-angle transient behavior. The numerical results for the various systems shown here correspond to sets of normalized parameters derived in the previous sections, with configurations A and B, using a value of $r = I/J = 0.1$. Allowing the tip mass weights to be limited to 5–25 lb, these parameters may be achieved for most practical spacecraft (3 to 1800 slug-ft^3), with booms ranging in length from 10 to 150 ft. Since steady-state behavior is, by design, confined to the small-angle regime, it can be conveniently characterized through the usual frequency-response representation, computed for the various possible sinusoidal excitations of the linear systems of Eqs. (2–25). Finally, the time histories of large-angle transients are used to illustrate the applicability of the derived control laws and to show deviations from the linear analysis.

Configuration A

The decoupling of the payload attitude motion from that of the reaction wheels and the boom is best illustrated in Fig. 3, showing the linear system response to initial errors of 1° in roll and yaw. The payload pointing errors are rapidly corrected. The motions of the boom are slowly damped yet show no significant amplification relative to the initial conditions. The effect of imperfect decoupling of the payload, produced by a small mismatch in control law parameters, is seen in Fig. 4. By violating the requirement of Eq. (10), and letting $(c_3 - c_5) = 0.1c_1$, the payload pitch axis is lightly coupled to the boom-wheel modes. A small amount of slowly damped libration at the "gravity-gradient" frequency $\omega \cong \Omega(3)^{1/2}$ appears on the payload. Typical frequency response characteristics (Fig. 5) are produced by exciting the linear system with a sinusoidal body-fixed torque having an

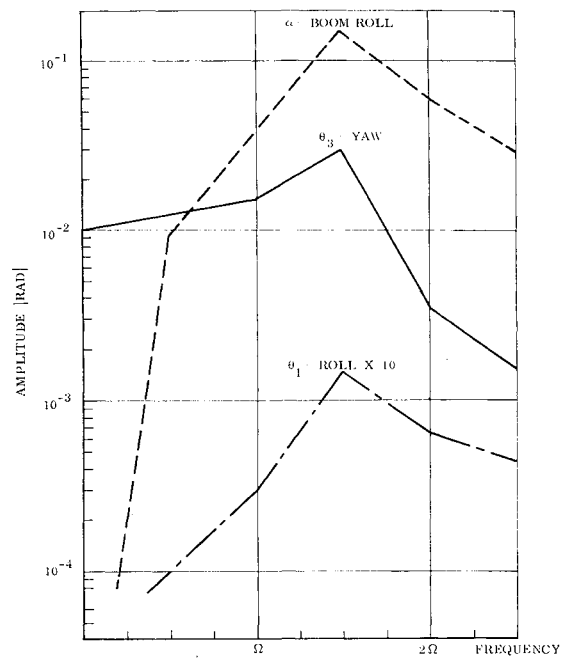

Fig. 11 Steady-state response amplitudes for configuration B for torque on payload yaw axis $T = I \times 10^{-6} \sin(n\Omega t)$ (ft-lb).

amplitude of 1×10^{-6} ft-lb, at frequencies $0 < \omega < 2.8\Omega$. Since the bandwidth associated with payload control is approximately an order of magnitude higher than the band of disturbance frequencies, the payload roll and yaw amplitudes remain small and constant. Note that the payload amplitudes are controlled primarily by the choice of k_1 of Eq. (8). The boom frequency response is essentially that of a damped, gravitationally stabilized dumbbell, peaking in the vicinity of $\omega \cong \Omega(3)^{1/2}$. The boom amplitudes depend primarily on the amount of damping and the boom-to-payload moment of inertia ratio. The introduction of slight coupling between boom and payload motion, corresponding to the case of Fig. 4, gives the frequency response of Fig. 6. Payload response amplitudes increase somewhat near the resonant frequency of the boom. Nevertheless, payload motion remains considerably smaller than that of the boom.

Figures 7 and 8 show representative large-angle response traces for configuration A, and illustrate an interesting aspect of reaction-boom system operation. Both runs use initial conditions of $\theta_2 = \theta_3 = 30°$. Figure 7 shows the usual rapid decay of the payload errors, with subsequent eventual damping of the boom and wheel motions. Figure 8 shows the system response with $\pm 25°$ stops imposed on both gimbals. It is seen that payload pointing is maintained only when the boom gimbals are off the stops. Thus, for large attitude errors, such as may occur during the initial deployment of the spacecraft, final attainment of the required payload pointing will, in general, be preceded by intermittent acquisition as seen in Fig. 8.

Configuration B

The small-angle transients for configuration B are shown in Figs. 9 and 10. The system has rapid responses to roll (and pitch) errors, but initial yaw conditions lead to the expected low frequency residual motion in roll and yaw. Typical steady-state response characteristics for the configuration are shown in Fig. 11. The inherent coupling between payload roll motion and an orbit-frequency mode is seen in the peaking of the payload response at $\omega \cong \Omega$. The passive control of payload yaw attitude also leads to somewhat increased sensitivity to yaw torques.

Concluding Remarks

The results presented here indicate strongly that continued development of analytical techniques and equipment for the reaction-boom methods should lead to a new class of control systems having both broad applicability and very favorable performance characteristics. The number of possible configurations is far greater than the examples used in this work. From the relative performance of configurations A and B, it is seen that the control capability of these systems depends strongly on the type and sophistication of the equipment used for sensing and actuation. Thus, further work should establish a variety of practical configurations, satisfying mission requirements ranging from simple 2-axis pointing to high-performance, large-angle maneuvering, with correspondingly varying equipment weight, power, and complexity.

Within the constraints of some of the simplifying assumptions made, reaction-boom systems provide performance competitive with other state-of-the-art control system types. At their best, they are capable of both fast maneuvering and steady-state pointing with sensor-limited accuracy of better than 0.1°. Working control laws can be developed using relatively straightforward linear analysis methods.

To provide a definitive analytical treatment of the reaction-boom concept, it is necessary to reconsider some of the simplifying assumptions used in the present work. Thus, future analysis efforts in this area should deal with the following: 1) analysis of boom flexibility effects: although early results[2] indicate that dynamic boom bending may not significantly affect system performance, the nonrigid nature of extendible booms must be evaluated to establish the associated limitations on spacecraft maneuvering rates and steady-state pointing in the presence of structural vibration. 2) Control law synthesis: the control laws derived in the present work represent the simplest forms which result in stable operation of the system. It is recognized that reaction booms, unlike reaction wheels, have an actuation capability which is dependent on both their attitude and their gimbal angles. Thus, to utilize fully the capability provided by a given number of control elements, it is necessary to consider the problem of control law selection more generally in terms of the reaction-torque and gravitational torque envelopes of the system. This approach may be expected to lead to both configuration synthesis methods and control law optimization procedures.

Finally, it is appropriate to comment briefly on the feasibility of mechanizing reaction-boom systems. It is clear that the required attitude sensors, control electronics, and reaction wheels (if any) are identical to those already in use in active control systems. Gimbal mechanizations with the associated flexures, torquers, and angle pickoffs do require specialized designs. However, these involve little more than standard equipment development and integration efforts.[2] Extendible booms are presently available in a variety of designs. Of these, the non-open-section, "zippered" types appear well suited for reaction-boom applications. Thus, the mechanization of reaction-boom control systems can be accomplished with state-of-the-art equipment and design methods.

References

[1] Gatlin, J. A. et al., "Satellite Attitude Control Using a Torqued, 2-Axis-Gimbaled Boom as the Actuator," *Journal of Spacecraft and Rockets*, Vol. 6, No. 9, Sept. 1969, pp. 1013–1018.

[2] Lloyd, W. B. et al., "A Hybrid Simulation Study of a Satellite Attitude Controller Using a Torqued, 2-Axis Gimbaled Boom as the Actuator," *Symposium on Gravity-Gradient Attitude Stabilization*, Aerospace Corp., El Segundo, Calif., Dec. 1968.

[3] Terasaki, R. M., "Dual Reaction Wheel Control for Spacecraft Pointing," *Symposium on Attitude Stabilization and Control of Dual-Spin Spacecraft*, Aerospace Corp., El Segundo, Calif., Aug. 1967.

[4] Hooker, W. W. and Margulies, G., "The Dynamical Attitude Equations for an n-Body Satellite," *Journal of the Astronautical Sciences*, Vol. 12, No. 4, Winter 1965, pp. 123–128.

[5] Hooker, W. W., "A Set of r Dynamical Attitude Equations for an Arbitrary n-Body Satellite Having r Rotational Degrees of Freedom," *AIAA Journal*, Vol. 8, No. 7, July 1970, pp. 1205–1207.